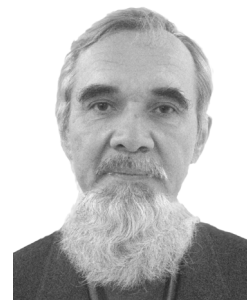

N.V. Morozova, V.V. Shchennikov



N.V. Morozova

Institute of Metal Physics, Ural Division of the Russian
Academy of Sciences, 18, S. Kovalevskaya Str.,
Yekaterinburg, 620990, GSP-170, Russia



V.V. Shchennikov

**THERMOELECTRIC POWER
OF RARE-EARTH METAL ROW OVER
A WIDE RANGE OF PRESSURES**

The results of investigations of thermoelectric properties of rare-earth metals under high pressure application up to 20 GPa at room temperature are reported. This study has experimentally confirmed that a high-pressure behavior of thermoelectric power of lanthanide metals follows a general trend due to the electron $s \rightarrow d$ transfer. A distinctive behavior of thermopower of divalent europium and ytterbium has been found under pressure application. Possible influence of valence change as well as the variation of the occupancy of s -, p -, d -electronic states under pressure on the behavior of the thermoelectric power of europium and ytterbium is discussed.

Key words: thermopower, high pressure, rare-earth metals.

Introduction

Thermoelectric effect (Seebeck effect, S) is a very efficient tool to study the electronic structure modification of materials at the variations of temperature (T) [1, 2] or pressure (P) [3]. The $S(P)$ data allow studying phase transitions as well as thermoelectric properties of high-pressure phases. The study of $S(P)$ of the rare-earth metals group allows summarizing the contribution of f - and d -states to the electron structure near the Fermi level over a wide range of pressures.

The range of applications of rare-earth metals is extraordinarily wide, from the petroleum cracking catalysts and pigments for glass and ceramics to the miniature nuclear batteries, superconductors and miniature magnets. So the knowledge of their electronic properties under stress application is critically important for technologies.

Rare-earth metals include the fifteen lanthanides as well as yttrium and scandium. Under high pressure most rare-earth metals suffer a sequence of phase transformations as follows: hcp \rightarrow Sm -type \rightarrow dhcp \rightarrow fcc \rightarrow distorted-fcc (d -fcc) [4-6]. This tendency involves the majority of rare-earth metals (Sc , Y , La , Pr , Nd , Pm , Sm , Gd , Tb , Dy , Ho , Er , Tm , and Lu). While some of them (Ce , Eu , and Yb) demonstrate very peculiar behavior.

The purpose of the present work is the investigation of the thermoelectric power of the rare-earth metal row under high pressure up to 20 GPa. The results of investigations of thermoelectric properties of typical lanthanides (Gd , Tb , Dy) that follow a commonly accepted sequence of structural transformations as well as peculiar ones: lanthanum (La), europium (Eu) and ytterbium (Yb) are presented. The latter metals have also peculiar electronic configurations: trivalent La has empty f -band and divalent Eu and divalent Yb possess one-half filled and completely filled $4f$ electron shell, respectively.

Experimental details

The experiments were carried out on pure polycrystalline samples of the rare-earth metals. Purity of the samples was as follows: *Sc* (99.9 %), *Y* (99.9 %), *La* (99.9 %), *Ce* (99.84 %), *Pr* (99.81 %), *Nd* (99.65 %), *Sm* (99.77 %), *Eu* (99.89 %), *Gd* (99.91 %), *Tb* (99.79 %), *Dy* (99.85 %), *Ho* (99.90 %), *Er* (99.91 %), and *Yb* (99.85 %). The measurements were performed on disk-shaped samples of $\sim 200 \mu\text{m}$ in the diameter and $\sim 30 \mu\text{m}$ in the thickness cut from the bulk ingots. Several samples of each element were examined one by one in the same conditions for verification of data reproducibility [7].

$S(P)$ measurements were carried out using the automated setup operating with high-pressure cells with synthetic diamond anvils [3]. A sample was loaded in a container made of the lithographic stone (soft CaCO_3 based mineral) that served both as a gasket and a pressure-transmitting medium. The ratio of container thickness (h) to a diameter of the top of diamond anvils $d = 600 \mu\text{m} \cdot h/d < 0.055$ provides the quasi-hydrostatic condition of pressure created [3, 8, 9]. The automated measurements permit obtaining high-quality data on pressure evolution of the thermoelectric properties. A good agreement has been obtained between the values of S at ambient pressure [2] and those measured on high-pressure setup at $P \approx 0$ GPa. The details of high-pressure experiments are described in the previous works [3, 7-9].

Results

A representative set of the data obtained is shown in Figure 1. Tables 1 and 2 summarize structural and thermoelectric data for the investigated rare-earth metals.

Table 1

*Structural and thermoelectric properties of the selected rare-earth metals
in the pressure range below 20 GPa*

Element	Z	Electronic configuration	Ambient structure	Phase transition pressures (GPa) from Refs. [4, 10-40]					
				<i>Sm</i> -type	dhcp	fcc	<i>d</i> -fcc	hcp	bcc
<i>La</i>	57	$4f^0(5d6s)^3$	dhcp	–	–	2 – 3	5.3 – 7	–	–
<i>Eu</i>	63	$4f^7(5d6s)^2$	bcc	–	–	–	–	12 – 14	–
<i>Gd</i>	64	$4f^7(5d6s)^3$	hcp	1 – 3.5	6.5 – 10	–	–	–	–
<i>Tb</i>	65	$4f^9(5d6s)^3$	hcp	3 – 5	12 – 16	–	–	–	–
<i>Dy</i>	66	$4f^{10}(5d6s)^3$	hcp	5 – 7.5	15 – 19	–	–	–	–
<i>Yb</i>	70	$4f^{14}(5d6s)^2$	fcc	–	–	–	–	–	3.5 – 4.5

Gadolinium, terbium and dysprosium crystallize in hcp lattice at ambient conditions. They show the standard transformation sequence: hcp \rightarrow *Sm*-type \rightarrow dhcp (Table 1). For gadolinium phase transitions occur at 1 – 3.5 and 6.5 – 10 GPa, respectively [4, 10-16] (Table 1). For terbium the same phase transitions occur at higher pressures 3 – 5 and 12 – 16 GPa [4, 10-12, 17, 18] (Table 1). And in dysprosium similar transition pressures are shifted to higher magnitudes, 5 – 7.5 and 15 – 19 GPa, respectively [4, 10, 12, 19-21] (Table 1). At room temperature, *Gd* exhibits also a ferromagnetic transition near 3.5 – 5 GPa [12, 22]. Ambient thermopower values were reported to be $S \sim -(0.7 \div 2) \mu\text{V/K}$,

$\sim -(0.9 \div 1.4) \mu\text{V/K}$, and $\sim -(0.55 \div 2) \mu\text{V/K}$ for *Gd*, *Tb* and *Dy*, respectively [2, 41] (Table 2). They agree well with our experimental data (Figs. 1, 2). Peculiarities detected on pressure dependence of thermoelectric power were referred to the above mentioned structural transitions. The Seebeck effect in gadolinium, terbium and dysprosium subjected to compression demonstrates similar behavior: monotonic rising from small negative values, $-(1 \div 2) \mu\text{V/K}$ to magnitudes of $\sim +(8 - 10) \mu\text{V/K}$ beyond ~ 5 GPa (Figs. 1, 2).

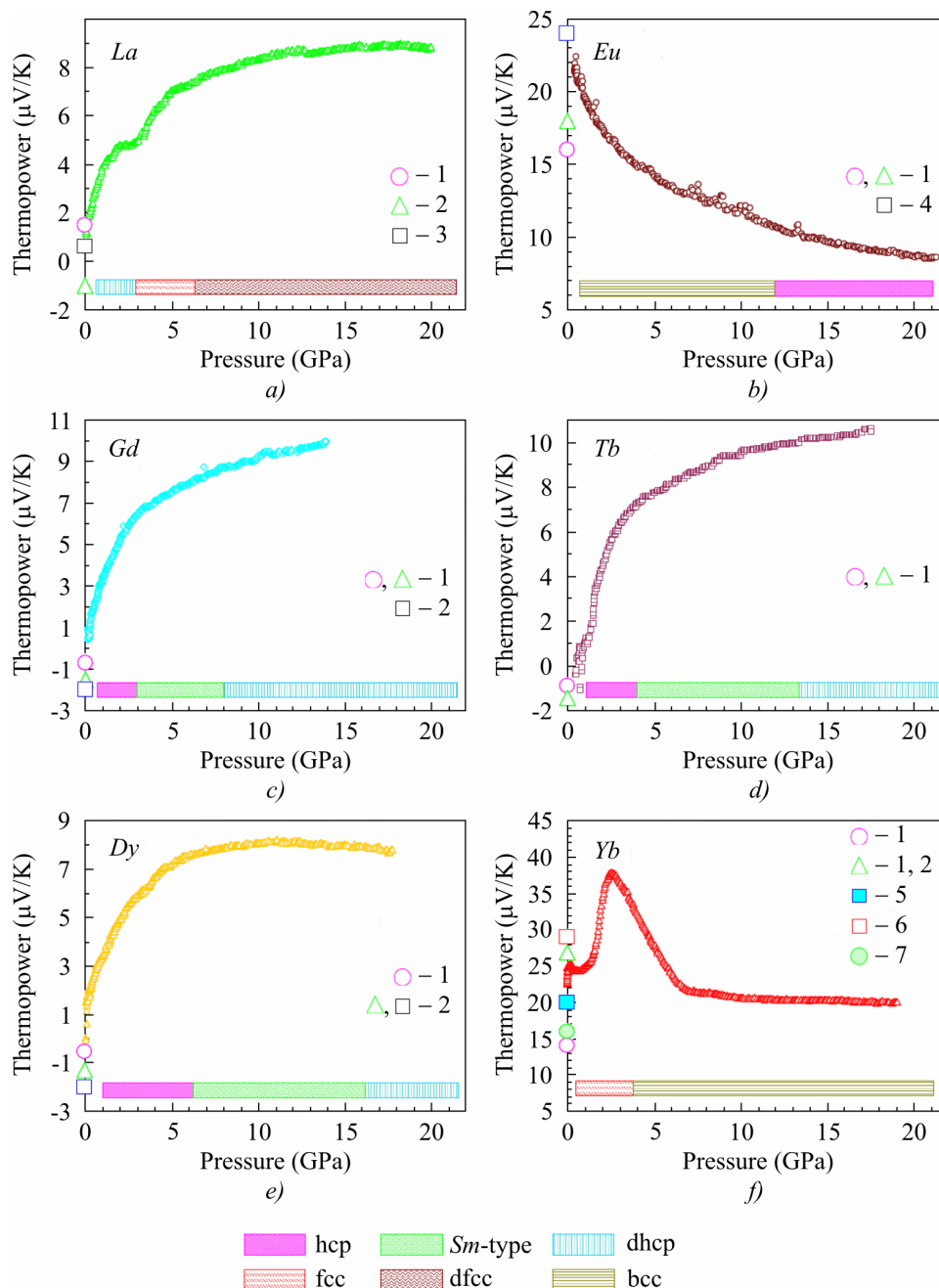


Fig. 1. Pressure dependencies of thermoelectric power of the selected lanthanides: (a) lanthanum, (b) europium, (c) gadolinium, (d) terbium, (e) dysprosium and (f) ytterbium.

The dashed rectangles schematically show the stability regions of different phases, summarized in Table 1.

The points 1 – 7 at ambient pressure label data taken from the literature: 1 – [2], 2 – [41], 3 – [42], 4 – [43], 5 – [39], 6 – [44], and 7 – [40]. Data for *Gd*, *Tb* and *Dy* have been taken from [7].

Table 2

Thermoelectric properties of the selected rare-earth metals
 in the range of pressures below 20 GPa

Element	Thermoelectric power ($\mu\text{V/K}$)	
	Ambient	at 16 – 20 GPa
<i>La</i>	+1.5 ^a , -1 ^b , +0.6 ^c	+8.9
<i>Eu</i>	+16 ^a , +18 ^a , +24 ^d	+8.5
<i>Gd</i>	-0.7 ^a , -1.5 ^a , -2 ^b	+(9.5 ÷ 10)
<i>Tb</i>	-0.9 ^a , -1.4 ^a , -1.2 ^b	+(10 ÷ 10.5)
<i>Dy</i>	-0.55 ^a , -1.3 ^b , -2 ^b	+8
<i>Yb</i>	+14 ^a , +27 ^{a, b} , +20 ^e , +29 ^f , +16 ^g	+20

^a – [2], ^b – [41], ^c – [42], ^d – [43], ^e – [39], ^f – [44], ^g – [40]

Lanthanum has $4f^0(5d6s)^3$ electronic configuration and at ambient conditions it crystallizes in a dhcp lattice (space group $P6_3/mmc$). It shows a phase transformation path: dhcp \rightarrow fcc \rightarrow distorted-fcc at 2 – 3 GPa and 5.3 – 7 GPa, respectively [4, 10, 23-26]. Ambient thermopower values determined in our experiments $S \cong (-1 \div +1.7) \mu\text{V/K}$ (Figs. 1(a) and 2) agree well with the literary data [2, 41, 42]. Pressure behavior of thermopower in *La* resembles those of most of the lanthanides [7], *Sc* and *Y* [45]. But on $S(P)$ dependence for *La* one can see a pronounced kink near 3 GPa related probably to the dhcp \rightarrow fcc transition [4, 10, 23-26]. A smooth bend in the thermopower curve near 5.5 – 6 GPa (Fig. 1 (a)) could be due to the structural transition into the distorted-fcc phase [4, 10, 23-26].

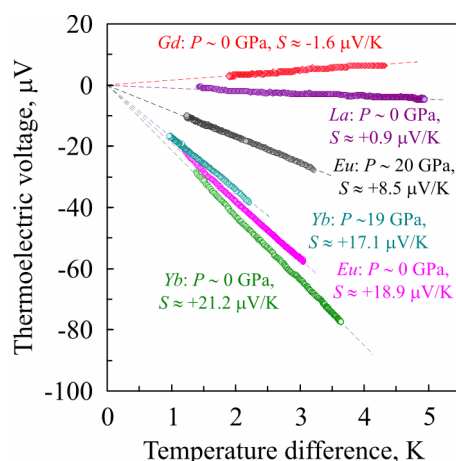


Fig. 2. Examples of dependences of thermoelectric signal U on applied temperature difference ΔT between sample edges. The values of thermopower S correspond to a linear coefficient between thermoelectric voltage (U) and temperature difference (ΔT) as follows: $S = -U/\Delta T$.

Europium is a divalent metal having an electron configuration of $4f^7(5d6s)^2$ and at ambient conditions, it adopts a body-centered cubic (bcc) lattice (space group $Im\bar{3}m$). At pressure of 12 – 14.5 GPa at room temperature, *Eu* transforms to hcp phase [4, 10, 27-32]. Previous studies have reported *Eu* to transform from the hcp structure to a new phase, *Eu*-III, at 18 GPa [4, 10, 30, 32]. However, recent *X*-ray diffraction investigations show a sluggish transition above 18 GPa to a mixture

of hcp and a monoclinic phase with space group $C2/c$ [29]. In [28, 30] it is illustrated that this Eu -III phase consists of hcp- Eu plus a rhombohedral phase (perhaps a hydride EuH_x), the atomic volume of which suggests that it is an impurity [28, 30]. At ambient pressure the thermopower values of Eu were found to be within a range of $S \sim (+17, +23) \mu\text{V/K}$ (Figs. 1 (b) and 2) close to previously reported values [2, 43]. The Seebeck effect decreases with pressure and reaches $S \sim +(8 \div 9) \mu\text{V/K}$ near 22 GPa (Figs. 1 (b) and 2). The pressure dependence of thermopower for this element (Fig. 1 b) is completely opposite to similar dependences for the majority of lanthanides [7].

Ytterbium is a divalent semimetal having an electron configuration of $4f^{14}(5d6s)^2$. At room and elevated temperatures, Yb has a fcc lattice (β -phase) of the $Fm\bar{3}m$ space group [10, 46-47]. With pressure application, it suffers fcc \rightarrow bcc phase transition at 3.5 – 4.5 GPa [4, 10, 33-40]. Near 2 GPa, Yb shows a semimetal-semiconductor electronic transition [39, 48-52]. A huge peak on the thermopower curve near 2.6 GPa (Fig. 1 (f)) is probably due to this electronic transition [39, 48-52]. With transition to the bcc lattice, Yb is reported to be metallized under pressure [10, 35, 36]. Ambient thermopower values were found to be $S \sim +(20 \div 25) \mu\text{V/K}$ (Figs. 1 (f) and 2), that is close to previously reported values [2, 39-41, 44].

Discussion

Similar thermopower behavior under pressure of lanthanides that follows a commonly accepted sequence of structural transformations [4] was observed in previous investigation [7]. For Sc , Y and La as well as for most of the lanthanides [7] the pressure applied tends to rising of the Seebeck effect to relatively high positive values of $S \sim 10 \mu\text{V/K}$ beyond $\sim 3 - 10$ GPa (not shown at Fig. 1). Divalent elements Eu and Yb do not follow a commonly observed sequence of structural transformations for lanthanides and also demonstrate pressure evolution of thermoelectric properties (Fig. 1) distinguishing from the above mentioned trend. Both metals have much higher initial values of $S \sim +25 \mu\text{V/K}$ which are strongly decreased under pressure in the bcc crystal structure (for Yb above ~ 3 GPa).

Under high pressure, a population of s -electrons in general decreases and that of d -electrons increases due to $s \rightarrow d$ electron transfer [4-6]. For a description of the thermopower behavior the expression ought to be used that takes contributions of both s - and d -bands into consideration [53]

$$S_d^s = -\frac{\pi^2 k^2 T}{3|e|} \left(\frac{3}{2\varepsilon} - \frac{1}{N_d(\varepsilon)} \frac{dN_d(\varepsilon)}{d\varepsilon} \right)_{\varepsilon=\varepsilon_F}, \quad (1)$$

where S_d^s is the diffusion thermoelectric power, k is the Boltzmann constant, T is the absolute temperature, e is the electron charge, ε is the electron energy, N_d is the density of states in the d -band and ε_F is the Fermi energy. Due to high concentrations of charge carriers in metals, the first term in Eq. 1 usually gives contributions to thermopower values of about $\sim 1 \mu\text{V/K}$. Thus, the higher thermopower values can not be explained by the first term and therefore they could come out from the second one. Similar behavior of thermoelectric properties of Gd , Tb , Dy and La under compression indeed can originate from pressure-enhanced scattering of the s -electrons by the carriers of d -band (the second term in Eq. 1). Most of lanthanides (except for Ce , Eu and Yb) demonstrate behavior of thermopower under pressure similar to La [7]. The contribution of the f -band to the values of S in view of similarity of $S(P)$ dependences for these rare-earth metals row seems to be not very essential [53].

The second term in Eq. 1 gives a positive contribution to S for almost empty d -band [53] that agrees well with our experiments (Figs. 1, 2)

The anomalous behavior of Eu and Yb thermopower under pressure may be due to several reasons. First, it may be partial delocalization of f -electrons and the corresponding increase of valence from 2 to 3. The second reason may be the variation of occupancy of s -, p -, d -electronic bands, and in particular the filling of almost empty d -bands. Peculiar electronic properties of Yb under pressure are believed to be determined by partial delocalization of the f -electrons [4-6, 14]. At higher pressures the narrow f -bands overlap and their interatomic interactions increase, finally leading to f -delocalization [14]. The fcc to bcc transition at Yb was proposed to occur when the $4f$ electrons start to delocalize varying the valence of Yb from $2+$ to $3+$ [39].

Experimental investigation of X -ray absorption near-edge spectroscopy (XANES) at Eu 's L_3 edge to pressures as high as 34 GPa [54], the ^{151}Eu Mössbauer spectroscopy studies to 14 GPa at 44 K [55] and synchrotron Mössbauer experiment at ambient temperature [56] have shown that the valence of Eu increases sharply under pressure, reaching the valence of ~ 2.5 at 10 – 12 GPa. A more recent XANES, X -ray magnetic circular dichroism, and synchrotron Mössbauer spectroscopy experiments have shown Eu metal to remain nearly divalent to the highest pressures reached (87 GPa) with magnetic order persisting to at least 50 GPa [57]. An analysis based on ab initio calculations indicates that the pressure-induced changes in XANES spectra in the 10 – 20 GPa range, which were previously interpreted as indicative of a marked change in Eu valence, result from significant changes in the electronic and crystal structure at the bcc \rightarrow hcp structural phase transition. However, this increase may originate from pressure-induced changes in the properties of the s -, p -, and d -electrons, and so is not related to a significant change in $4f$ -electron occupation. Thus, Eu metal probably remains divalent or nearly divalent to 87 GPa [57]. Using the second approach of change in the occupancy of electronic s -, p -, d -states, the strong decrease of S in Eu with a rise in pressure is attributable to considerable increase of s -electron states density (and hence the electron concentration) or to filling of empty d -band; with certain occupancy of d -band the second term in Eq.1 is reduced indeed [53].

Conclusions

The measurements of thermoelectric power of rare-earth metals over a wide range of pressures have revealed the similarity of $S(P)$ behavior for most members of the row (except for Ce , Eu and Yb) corresponding to similarity of the sequence of structural transformations under pressure of these metals. For divalent Yb and Eu the inverse pressure dependence of S (decrease) in bcc phase as compared to the rest of rare-earth metals can be attributed to several possible reasons: the partial delocalization of f -states (most probably it occurs at Yb) [4-6, 14, 39] and the variation of occupancy of s -, p -, d -electron bands [57]. The second term in Eq. 1 indeed has a sharp maximum at certain position of the Fermi level [53] that may tend to decrease in S with a rise in pressure. The second approach also allows explaining the high values of $S \sim +25 \mu\text{V/K}$ for Yb and Eu as compared to the rest of rare-earth metals.

The work was done within RAS Program (Project no. 01.2.006 13394), by UD RAS as part of Program “Matter at high energy densities” of the Presidium of RAS (project 12-P-2-1004), by the Ministry of Education and Science of the Russian Federation (Contract 14.518.11.7020), and by the Oriented Basic Research Project of the Ural Branch of the Russian Academy of Sciences.

References

1. M.V. Vedernikov, The Thermoelectric Powers of Transition Metals at High Temperature, *Advances in Physics* **18** (74), 337 – 370 (1969).
2. I.V. Vedernikov, A.T. Burkov, V.G. Dvinitkin, and N.I. Moreva, The Thermoelectric Power, Electrical Resistivity and Hall Constant of Rare Earth Temperature Range 80-1000 K, *Journal of the Less-Common Metals* **52**, 221 – 245 (1977).
3. V.V. Shchennikov, S.V. Ovsyannikov, and A.Y. Manakov, Measurement of Seebeck Effect (Thermoelectric Power) at High Pressure up to 40 GPa, *J. Phys. Chem. Solids* **71** (8), 1168 – 1174 (2010).
4. W.B. Holzapfel, Physics of Solids under Strong Compression, *Rep. Prog. Phys.* **59**, 29 – 90 (1996).
5. B. Johansson, A. Rosengren, Generalized Phase Diagram for the Rare-Earth Elements: Calculations and Correlations of Bulk Properties, *Phys. Rev. B* **11** (3), 2836 – 2857 (1975).
6. J.C. Duthie, D.G. Pettifor, Correlation between *d*-Band Occupancy and Crystal Structure in the Rare Earths *Phys. Rev. Lett.* **38** (10), 564 – 567 (1977).
7. V.V. Shchennikov, N.V. Morozova, and S.V. Ovsyannikov, Similar Behavior of Thermoelectric Properties of Lanthanides under Strong Compression up to 20 GPa, *J. Appl. Phys.* **111**, 112624 (2012).
8. S.V. Ovsyannikov, V.V. Shchennikov, A. Misiuk, and I.A. Komarovskiy, Electronic Properties and Phase Transitions in *Si*, *ZnSe*, and *GaAs* under Pressure Cycling up to 20 – 30 GPa in a High-Pressure Cell, *Physica Status Solidi B* **246** (3), 604 – 611 (2009).
9. S.V. Ovsyannikov, V.V. Shchennikov, High-Pressure Routes in the Thermoelectricity or How One Can Improve a Performance of Thermoelectrics, *Chem. Mater.* **22**, 635 – 647 (2010).
10. E.Yu. Tonkov, E.G. Ponyatovsky, *Phase Transformations of Elements under High Pressure* (Washington, CRC Press, 2004), 377 p.
11. M. Mito, K. Matsumoto, Y. Komorida, H. Deguchi, S. Takagi, T. Tajiri, T. Iwamoto, T. Kawae, M. Tokita, and K. Takeda, Volume Shrinkage Dependence of Ferromagnetic Moment in Lanthanide Ferromagnets Gadolinium, Terbium, Dysprosium, and Holmium, *J. Phys. Chem. Solids* **70**, 1290 – 1296 (2009).
12. D.B. McWhan, A.L. Stevens, Effect of Pressure on the Magnetic Properties and Crystal Structure of *Gd*, *Tb*, *Dy*, and *Ho*, *Phys. Rev.* **139**, A682 – A689 (1965).
13. A. Nakaue, Studies in the Pressure-Temperature Phase Diagram of *Nd*, *Sm*, *Gd* and *Dy*, *J. Less-Common Met.* **60**, 47 – 58 (1978).
14. H. Olijnyk, Lattice Vibrations and Electronic Transitions in the Rare-Earth Metals: Yttrium, Gadolinium and Lutetium, *J. Phys.: Condens. Matter* **17**, 43 – 52 (2005).
15. J. Akella, G.S. Smith, and A.P. Jephcoat, High-Pressure Phase Transition Studies in Gadolinium to 106 GPa, *J. Phys. Chem. Solids* **49**, 573 – 576 (1988).
16. W.A. Grosshans, W.B. Holzapfel, Atomic Volumes of Rare-Earth Metals under Pressures to 40 GPa and above, *Phys. Rev. B* **45** (10), 5171 – 5178 (1992).
17. N.C. Cunningham, W. Qiu, K.M. Hope, H.-P. Liermann, and Y.K. Vohra, Symmetry Lowering under High Pressure: Structural Evidence for *f*-Shell Delocalization in Heavy Rare Earth Metal Terbium, *Phys. Rev. B* **76**, 212101 (2007).
18. J.S. Olsen, S. Steenstrup, and L. Gerward, High Pressure Phases of Terbium: Possibility of a *thcp* Phase, *Phys. Lett. A* **109**, 235 – 237 (1985).
19. J.C. Jamieson, X-ray Diffraction Studies on Dysprosium at High Pressures, *Science* **145**, 572 – 574 (1964).

20. Y.R. Shen, R.S. Kumar, A.L. Cornelius, and M.F. Nicol, High-Pressure Structural Studies of Dysprosium using Angle-Dispersive X-ray Diffraction, *Phys. Rev. B* **75**, 064109 (2007).
21. J.R. Patterson, C.K. Saw, and J. Akella, Static High-Pressure Structural Studies on Dy to 119 GPa, *J. Appl. Phys.* **95**, 5443 – 5446 (2004).
22. N. Tateiwa, A. Nakagawa, T. Iwamoto, T. Kawae, M. Hidaka, K. Takeda, and M. Mito, Electrical Resistance Measurement on a Ferromagnetic Element Gadolinium under High Pressure, *J. Magn. Magn. Mater.* **272-276**, 34 – 35 (2004).
23. F. Porsch, W.B. Holzapfel, Novel Reentrant High Pressure Phase Transition in Lanthanum, *Phys. Rev. Lett.* **70** (26), 4087 – 4089 (1993).
24. H. Bohn, A. Eichler, Specific Heat of d-hcp and fcc Lanthanum under High Pressure, *Z. Phys. B – Condensed Matter* **83**, 105 – 111 (1991).
25. G.Y. Gao, Y.L. Niu, T. Cui, L.J. Zhang, Y. Li, Y. Xie, Z. He, Y.M. Ma, and G.T. Zou, Superconductivity and Lattice Instability in Face-Centered Cubic Lanthanum under High Pressure, *J. Phys.: Condens. Matter* **19**, 425234 (2007).
26. V.A. Goncharova, G.G. Il'ina, Anomalies in the Elastic Properties of Polycrystalline Lanthanum at Phase Transitions under Pressure, *Zh. Eksp. Teor. Fiz.* **86**, 1708 – 1714 (1984).
27. R.J. Husband, I. Loa, G.W. Stinton, S.R. Evans, G.J. Ackland, and M.I. McMahon, Europium-IV: An Incommensurately Modulated Crystal Structure in the Lanthanides, *Phys. Rev. Lett.* **109**, 095503 (2012).
28. R.J. Husband, I. Loa, G.W. Stinton, S.R. Evans, G.J. Ackland, and M.I. McMahon, The Structure of Eu-III, *J. Phys.: Conf. Ser.* **377**, 012030 (2012).
29. W. Bi, Y. Meng, R.S. Kumar, A.L. Cornelius, W.W. Tipton, R.G. Hennig, Y. Zhang, C. Chen, and J.S. Schilling, Pressure-Induced Structural Transitions in Europium to 92 GPa, *Phys. Rev. B* **83**, 104 – 106 (2011).
30. R.J. Husband, I. Loa, G.W. Stinton, G.J. Ackland, and M.I. McMahon, Phase Transitions in Europium at High Pressures, *High Pressure Research* **33**(1), 158 – 164 (2013).
31. W.A. Grosshans, W.B. Holzapfel, X-ray Studies on Europium and Ytterbium up to 40 GPa, *J. Magn. Magn. Mater.* **47&48**, 295 – 296 (1985).
32. K. Takemura, K. Syassen, Pressure-Volume Relations and Polymorphism of Europium and Ytterbium to 30 GPa, *J. Phys. F: Met. Phys.* **15**, 543 – 559 (1985).
33. W.H. Gust, E.B. Royce, New Electronic Interactions in Rare-Earth Metals at High Pressure, *Phys. Rev. B* **8** (8), 3595 (1973).
34. B.I. Min, H.J.F. Jansen, T. Oguchi, A.J. Freeman, Electronic and Structural Properties of Rare Earth Metals at Normal and High Pressures: Eu and Yb, *J. Magn. Magn. Mater.* **59**, 277 – 286 (1986).
35. R.H. Mutlu, Calculated High-Pressure-Induced Electronic and Structural Phase Transitions in Sr and Yb up to 50 kbar, *Phys. Rev. B* **54**, 16321 – 16324 (1996).
36. D.B. McWhan, T.M. Rice, and P.H. Schmidt, Metal-Semiconductor Transition in Ytterbium and Strontium at High Pressure, *Phys. Rev.* **177**, 1063 – 1071 (1969).
37. G.N. Chesnut, Y.K. Vohra, Structural and Electronic Transitions in Ytterbium Metal to 202 GPa, *Phys. Rev. Lett.* **82**, 1712 – 1715 (1999).
38. Y.C. Zhao, F. Porsch, and W.B. Holzapfel, Irregularities of Ytterbium under High Pressure, *Phys. Rev. B* **49**, 815-817 (1994).
39. N.V.C. Shekar, J.F. Meng, D.A. Polvani, and J.V. Badding, Thermoelectric Power of Nickel and Ytterbium at High Pressure: a Comparative Study, *Solid State Communications* **116**, 443 – 445 (2000).

40. A.O. Saburov, N.N. Stepanov, A.P. Shvetsov, Thermoelectric Power of Yb under Hydrostatic Pressures up to 11 GPa, *Solid State Physics* **32** (8), 2497 – 2500 (1990).
41. H.J. Born, S. Legvold, F.H. Spedding, Low-Temperature Thermoelectric Power of the Rare-Earth Metals, *J. Appl. Phys.* **32**, 2543 – 2549 (1961).
42. V. Vijakumar, Investigation of Pressure Induced Electronic Transitions in Lanthanum, Uranium and Thorium, *Journal of Physics and Chemistry of Solids* **46** (1), 17 – 20 (1985).
43. G.T. Meaden, N.H. Sze, Thermoelectric Power of Annealed and Strained Europium Metal Between 10 and 300°K, *Journal of Low Temperature Physics* **1** (6), 568 – 576 (1969).
44. M.A. Angadi, P.V. Ashrit, Thermoelectric Effect in Ytterbium and Samarium Films, *J. Phys. D: Appl. Phys.* **14**, L125-8 (1981).
45. V.V. Shchennikov, N.V. Morozova, and S.V. Ovsyannikov, Thermoelectric Properties of Rare-Earth Elements at High Pressures, *Program and Book of Abstracts of 50th European High Pressure Research Group Meeting* (Thessaloniki, Greece, 2012), p. 157.
46. E. Bucher, P.H. Schmidt, A. Jayaraman, K. Andres, J.P. Maita, K. Nassau, and P.D. Dernier, New First-Order Phase Transition in High-Purity Ytterbium Metal, *Phys. Rev. B* **2**(10), 3911 – 3917 (1970).
47. H.T. Hall, J.D. Barnett, L. Merrill, Ytterbium: Transition at High Pressure from Face-Centered Cubic to Body-Centered Cubic Structure, Reprinted from *Science* **139** (3550), 111 – 112 (1963).
48. L. Spendeler, D. Jaccard, and J. Sierro, High Pressure Transport Properties of Pure Ytterbium in the Metallic bcc Phase, *Physics Letters A* **177**, 375 – 378 (1993).
49. T.G. Ramesh, V. Shubha, S. Ramaseshan, Phase Transitions in Ytterbium under Pressure, *J. Phys. F: Metal Phys.* **7** (6), 981 – 990 (1977).
50. H. Katzman, J.A. Mydosh, High-Pressure Resistance-Temperature Behavior of bcc-Ytterbium, *Z. Physik* **256**, 380 – 386 (1972).
51. C.M. Hurd, J.E.A. Alderson, Another Indicated Phase Transformation in Ytterbium, *Solid State Communications* **12**, 375 – 377 (1973).
52. B.J. Beaudry, K.A. Gschneidner Jr., Concerning another Indicated Phase Transition in Ytterbium, *Solid State Communications* **15**, 791 – 793 (1974).
53. F.J. Blatt, P.A. Schroeder, C.L. Foiles, and D. Greig, *Thermoelectric Power of Metals* (New York Plenum, 1979), 264 p.
54. J. Röhler, The Valence of Eu under High Pressure, *Physica* **144B**, 27 – 31 (1986).
55. R.D. Taylor, J.N. Farrell, Mössbauer Effect of Europium Metal under Pressure, *J. Appl. Phys.* **61**, 3669 (1987).
56. G. Wortmann, U. Ponkratza, B. Bielemeiera, and K. Rupperecht, Phonon Density-of-States in bcc and hcp Eu Metal under High Pressure Measured by 151 Eu Nuclear Inelastic Scattering of Synchrotron Radiation, *High Pressure Research* **28** (4), 545 – 551 (2008).
57. W. Bi, N.M. Souza-Neto, D. Haske, G. Fabbris, E.E. Alp, J. Zhao, R.G. Hennig, M.M. Abd-Elmeguid, Y. Meng, R.W. McCallum, K. Dennis, J.S. Schilling, Synchrotron X-ray Spectroscopy Studies of Valence and Magnetic State in Europium Metal to Extreme Pressures, *Physical Review B* **85**, 205134 (2012).

Submitted 16.05.2013.